Available online at www.sciencedirect.com
SCIENCE DIRECT
Talanta 68 (2006) 1632–1639
Talanta
www.elsevier.com/locate/talanta

Platinum black coated microdisk electrodes for the determination of high concentrations of hydrogen peroxide in phosphate buffer solutions

Aleksandra Kicela, Salvatore Daniele *

Department of Physical Chemistry, University of Venice Calle Larga, S. Marta 2137, 30123 Venice, Italy

Received 18 April 2005; received in revised form 27 July 2005; accepted 9 August 2005
Available online 12 September 2005

Abstract

The performance of a series of platinum black coated microdisk electrodes (Pt-Bs) was investigated in H_2O_2 solutions over the concentration range 0.1–500 mM, in phosphate buffer media pH 7. The Pt-Bs were prepared by electrodeposition of Pt onto the surface of microdisk electrodes 12.5 μm of nominal radius, from aqueous solutions containing hexachloroplatinic acid. The resulting roughness factors (RF, i.e., the ratio of the effective surface area to the geometric electrode area) varied between about 10 and 100. The voltammograms recorded with these electrodes, at relatively low H_2O_2 concentrations (up to 50–100 mM), displayed rather steep mixed anodic–cathodic waves, which attained well-defined and stable current plateaus. At the higher hydrogen peroxide concentrations, additional waves both in the anodic and cathodic region or dramatic current drop phenomena were observed. The wave split phenomenon was attributed to the insufficient buffering capacity of the base electrolyte solution within the pores of the platinum black, induced by the large amounts of hydrogen ions produced in the oxidation process. The current drop was attributed to either the formation of oxygen bubbles, which limit diffusion of H_2O_2 down the pores, or saturation of the active sites responsible for the decomposition of H_2O_2 to O_2 and H_2O. The H_2O_2 concentration at which the above phenomena occurred depended either on the phosphate buffer concentration in the bulk solution or the RF factor of the electrodes. The latter conditions also affected the dynamic range of detection, the sensitivity and low detection limits. Advantageous analytical characteristics were obtained with a Pt-B of RF of about 24, which provided a dynamic range between 0.5 and 230 mM, a sensitivity of 1.93(±0.06) A M^{-1} cm^{-2} and a low detection limit of 0.05 mM. The reproducibility was also very good, it being within 2–3%. The usefulness of the Pt-Bs for real samples analysis was tested in an antiseptic solution containing large amounts of H_2O_2.

Keywords: Hydrogen peroxide; High surface area; High concentration; Platinum black; Microelectrodes

1. Introduction

Hydrogen peroxide is a molecule of interest to many fields [1–6], and numerous reports have appeared on analytical methods for its determination [1–26]. Among them, electrochemical methods based on the measurement of current derived from H_2O_2 oxidation or reduction play a predominant role, especially in the topic of biosensors, as H_2O_2 is produced by the action of enzymes upon reaction with bio-substrates [27]. Different electrode systems, which include either simple metal electrodes such as platinum [16,23,28–32], gold [14,15,17], iridium [16,18] and palladium [17,18], or electrodes modified with enzymes [13,24–26,33–37] and Prussian Blue-type analogues [38–40] have been investigated. These electrodes, in some cases, have provided good performance in terms of sensitivity, dynamic range and low detection limits (down to 10 nM [37]). However, upper limits of detection achieved with these amperometric devices are of a few tens of millimolars (10–20 mM). Conditions for the rapid monitoring of H_2O_2 at higher concentration levels, which are demanding for control of some industrial processes [3,22], have been much less investigated.

The difficulties that arise in the amperometric determination of concentrated hydrogen peroxide solutions are mainly related to the complex nature of the electrode process

* Corresponding author. Tel.: +39 041 2348630; fax: +39 041 2348594.
E-mail address: sig@unive.it (S. Daniele).

0039-9140/$ – see front matter © 2005 Elsevier B.V. All rights reserved.
doi:10.1016/j.talanta.2005.08.023

involved. In particular, for metal electrodes, surface processes usually inhibit the overall electrode reaction. Considering platinum, which is probably the most employed electrode material, the current response to hydrogen peroxide is under mixed kinetic and diffusion control and further complicated by competitive adsorption of oxygen onto Pt active surface sites and the protonation of the adsorbed H_2O_2 complex species [28–32]. Therefore, a lack of Pt surface sites limits the rate of the electrode process and causes a current depression for higher H_2O_2 concentrations. High surface platinum black [41], and mesoporous platinum microelectrodes [42] have been used for H_2O_2 detection and an upper detection limit of 40 mM has been reported [41]. In principle, high surface Pt electrodes systems should circumvent the problems related to the limited number of active sites. However, to the best of our knowledge, no detailed study exists on their voltammetric performance in high concentrated solutions of H_2O_2.

In this paper we report the results of an investigation aimed at verifying to what extent platinum black coated platinum microdisk electrodes (Pt-B) could be used for the determination of H_2O_2 at high concentrations. These electrode systems should combine the high surface area of platinum black and the favourable properties of microelectrodes. In fact, platinum black electrodes are characterised by a specific surface area of about $21\,m^2\,g^{-1}$ [43], which should ensure a high number of surface sites for the H_2O_2 decomposition to O_2 and H_2O [44]. On the other hand, the enhanced mass transport and the achievement of steady-state conditions in short time, typical of microelectrodes [45], should make easier the analysis of experimental data, or minimise some of the inhibition effects due to the reaction products.

Platinum black coated microelectrodes with roughness factors (RF) (i.e., the ratio of the effective surface area to the geometric electrode area) varying from about 10 to 100 and, for comparison, an uncoated platinum microdisk with RF of about 4 are examined. The hydrogen peroxide concentration range investigated varies from 0.1 to 500 mM, and the measurements are performed in phosphate buffers pH 7, at concentrations varying between 0.2 and 2.5 M.

2. Experimental

2.1. Chemicals and materials

All chemicals employed were of analytical reagent grade. Hexachloroplatinic acid (HCPA), sulphuric acid, hydrogen peroxide (35% solution in water), potassium chloride were purchased from Aldrich. Sodium dihydrogen phosphate monohydrate and di-sodium hydrogen phosphate anhydrous were supplied by Fluka. Hexaammineruthenium (III) chloride was purchased from J. Matthey. All chemical were used as received. The antiseptic solution Oxonia Active, which is made by a mixture of peroxyacetic acid (48.6 wt.%), hydrogen peroxide (23 wt.%) and acetic acid (22 wt.%), was purchased from Henkel-Ecolab (Milano, Italy). For test measurements it was diluted with pure water 80–100-fold and then added of a proper amount of phosphate buffer to provide pH ≈ 7.

All aqueous solutions were prepared with deionised water purified via a Milli-Q unit (Millipore, Bedford, MA). All measurements were performed in solutions purged with pure nitrogen (99.99% from SIAD, Italy).

2.2. Electrodes and instrumentation

All electrochemical experiments were carried out in a two-electrode cell maintained in a Faraday cage made of sheets of aluminium to minimise external interference. The reference electrode was an Ag/AgCl saturated with KCl. In the platinum electrodeposition experiments and for the hydrogen under potential deposition (UPD) measurements, a platinum spiral was used as pseudo reference electrode (PtPRe). Working microelectrodes were prepared by sealing 12.5 μm radius platinum wires (Goodfellow, Cambridge Science Park, England) into glass capillary tubes. Prior to each series of measurements the smooth platinum microelectrodes were polished mechanically with aqueous suspension of alumina powder of different size 1, 0.3 and 0.05 μm supported on a microcloth polishing paths (Buehler, Lake Bluff, IL, USA), and then rinsed thoroughly with water. An electrochemical pre-treatment of the electrode surface was also accomplished. It consisted in cycling several times (three to five times) the potential from −1 to 2 V at $200\,mV\,s^{-1}$. In this way, oxide formation and reduction occurred which led to refreshing of the electrode surface [46].

The effective radii of the microdisks were determined by recording the steady-state diffusion limiting current (I_L) from a 1 mM $Ru(NH_3)_6Cl_3$ solution in milli-Q water containing 0.1 M KCl, and using the following equation [47]:

$$I_L = 4nFDc^b a \quad (1)$$

where n is the number of electrons, F the Faraday constant, D the diffusion coefficient of the electroactive species ($7.0 \times 10^{-6}\,cm^2\,s^{-1}$ [48]), c^b the bulk concentration and a is the radius of the microdisk.

Pt-Bs were prepared by electrodeposition of platinum onto the smooth platinum microdisks from a 50% HCPA aqueous solution. Platinum deposition was carried out under potentiostatic conditions at −0.6 V versus PtPRe. The amount of Pt deposited was controlled from the current–time profiles recorded during the plating step. In this way Pt-Bs with different surface area were prepared and characterised as described in the next section. A scanning electron microscopy (SEM) image of a Pt black deposit is shown in Fig. 1.

Cyclic voltammetry and chronoamperometry were performed by using the Potentiostat/Galvanostat M 283 EG&G PAR (Princeton, NY), and the M 270 electrochemical analysis software (EG & 8G PAR).

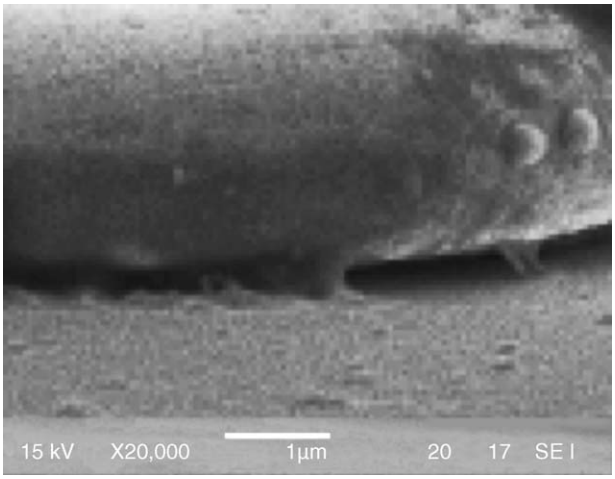

Fig. 1. SEM image of a typical Pt-black deposit.

All measurements were performed at room temperature, $22 \pm 1\,^{\circ}C$.

3. Results and discussion

3.1. Voltammetric characterisation of the platinum black microelectrodes

The electrochemical active surface areas of the Pt-Bs were evaluated by cyclic voltammetry in a 2 M H_2SO_4 aqueous solution, and exploiting the hydrogen UPD process [49,50]. Fig. 2 shows typical cyclic voltammograms obtained at 200 mV s^{-1} over the potential range from −0.3 to 0.7 V versus PtPRe, with a Pt-B (full line) and that of the corresponding smooth Pt microdisk before platinum deposition (dashed line). At both types of microelectrodes the typical voltammetric pattern expected for polycrystalline platinum is observed [50]. The larger current involved at the Pt-B is clearly due to the enhanced effective surface area, upon Pt deposition. From the hydrogen adsorption/desorption charge involved in the potential range from −0.4 to −0.3 V versus PtPRe (Fig. 2) (after the subtraction of the double layer charge, and assuming a monolayer of hydrogen corresponds to an adsorption of 210 µC/cm^2 [51]), the real surface areas of the Pt-Bs, and, for comparison, those of the corresponding smooth microdisks, were evaluated. These surface area values were divided for the corresponding geometric area to produce the RF values shown in Table 1. From this table it is evident that all Pt-Bs have the surface sensibly enhanced in comparison with the corresponding polished Pt electrodes.

Table 1
Roughness factors, steady-state limiting currents and radii of Pt microdisks before and after platinum black deposition

Smooth Pt			Pt-B		
RF	I_L (nA) (±0.05)	a (µm)	RF	I_L (nA) (±0.05)	a (µm)
3.6	3.51	12.9	97.1	4.45	16.5
1.7	3.40	12.6	23.4	3.46	12.8
4.7	3.38	12.5	32.0	3.70	13.7
3.2	3.41	12.6	50.5	3.84	14.2
2.7	3.37	12.5	10.1	3.43	12.7

In order to verify whether the diffusional characteristics of the microelectrodes were retained at the high surface Pt-Bs, a series of measurements was performed in a 1 mM $Ru(NH_3)_6^{3+}$ + 0.1 M KCl aqueous solution. Fig. 3 compares the cyclic voltammograms obtained at low scan rate at a Pt-B (RF = 32) and that of the corresponding smooth Pt microdisk. Both types of electrodes exhibit sigmoidal shaped waves in the forward and backward scan, which are typical for microelectrodes working under steady-state conditions [45]. This means that the non-uniform current density distribution to the microdisks was not affected by the platinum black deposit. However, the voltammogram obtained with the Pt-B displays a larger hysteresis, probably due to a larger double layer capacitance. Also, its diffusion-limiting current is larger than that of the smooth electrode, probably as a consequence of a slight lateral growth of the deposited platinum. Similar

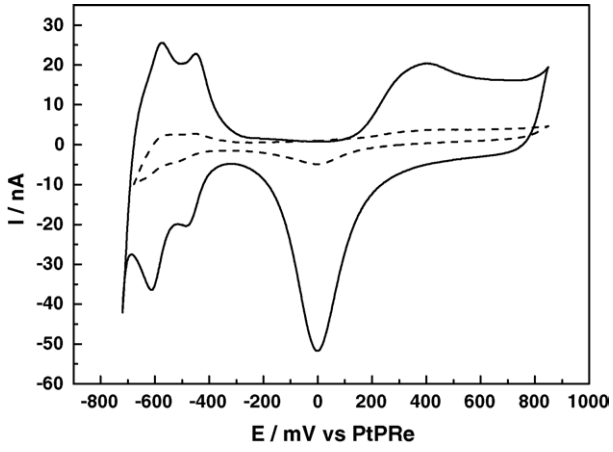

Fig. 2. Cyclic voltammograms recorded at 200 mV s^{-1} with Pt microdisks in 2 M H_2SO_4 solution: (a) smooth Pt 12.5 µm radius, and (b) Pt-B; RF = 32.

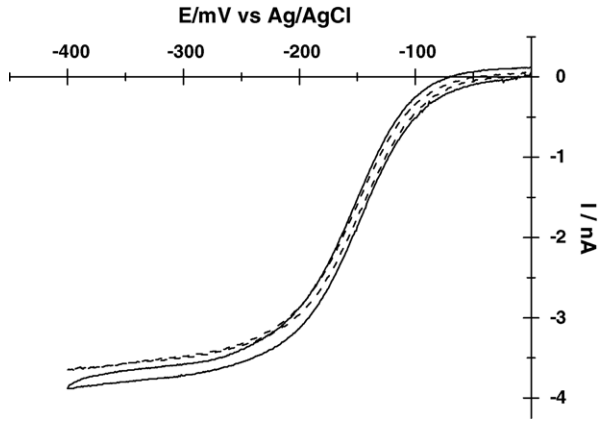

Fig. 3. Cyclic voltammograms recorded at 5 mV s^{-1} with Pt microdisks in 1 mM $Ru(NH_3)_6^{3+}$ containing 0.1 M KCl as supporting electrolyte. (- - -) Smooth Pt 12.5 µm radius, (—) Pt-B; RF = 32.

results were obtained with all Pt-Bs investigated; the hysteresis effects and the steady-state limiting currents were the higher the larger were the RF factors of the electrodes. From the steady-state limiting currents and Eq. (1), the radii of the microelectrodes were evaluated. Table 1 includes steady-state limiting currents and the calculated radii of the microelectrodes before and after platinum deposition. As expected, the radius of each Pt-B is larger than that of the corresponding smooth microdisk, and it is the bigger the greater the RF value.

3.2. Voltammetric behaviour of platinum black microelectrodes in H_2O_2 solutions

Fig. 4 shows typical cyclic voltammograms obtained with a Pt-B (RF = 32) at 20 mV s^{-1} over the potential range from −0.2 to 0.8 V (versus Ag/AgCl), in 0.2 M phosphate buffer containing H_2O_2 at different concentrations. The voltammograms recorded over the concentration range 1–50 mM (Fig. 4A, curves a–e and inset) present rather steep mixed anodic–cathodic waves, which attain well-defined and stable

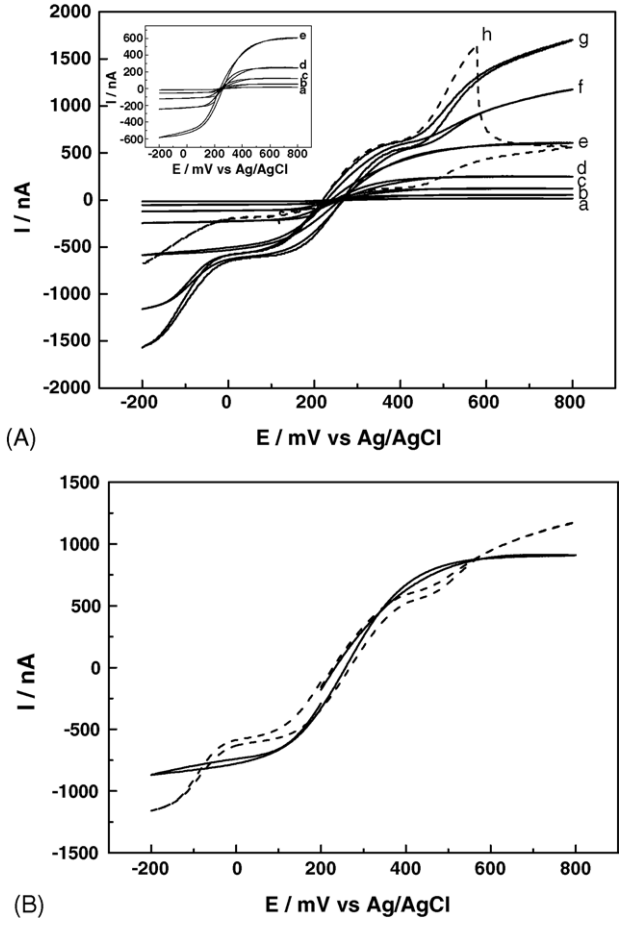

Fig. 4. Cyclic voltammograms recorded at 20 mV s^{-1} with a Pt-B, RF = 32—(A) 0.2 M phosphate buffer (pH = 7): (a) 1 mM, (b) 5 mM, (c) 10 mM, (d) 20 mM, (e) 50 mM, (f) 100 mM, (g) 150 mM, (h) 200 mM H_2O_2; (B) 100 mM H_2O_2 and (- - -) 0.2 M and (—) 1 M phosphate buffer (pH = 7). (Inset) As in (A), curves a–e.

current plateaus. The anodic and cathodic branches clearly correspond, respectively, to H_2O_2 oxidation and reduction, according to the following overall reactions [23]:

$$H_2O_2 \rightleftarrows O_2 + 2H^+ + 2e^- \quad (2)$$

$$H_2O_2 + 2e^- + 2H^+ \rightleftarrows 2H_2O \quad (3)$$

The steepness of the curves suggests that a rather fast apparent electron transfer rate is in any case operative. Moreover, the current–potential curves cross the zero current axis almost at the same potential: 0.250 ± 0.006 V versus Ag/AgCl, which compares well with the open circuit value of 0.244 V found previously in phosphate buffer solutions containing H_2O_2 [31]. Thus, at the latter potential the decomposition of H_2O_2 to O_2 and H_2O occurs to a significant extent [23,42].

Increasing the hydrogen peroxide concentration, the voltammetric pattern changed as shown in Fig. 4A (curves f–h). In particular, for H_2O_2 concentrations above about 80 mM and below 200 mM, both anodic and cathodic waves split (curves f and g), though the overall currents at more anodic and cathodic potentials still increase as H_2O_2 concentration is increasing. The shape of the additional waves, especially that in the anodic region, are more drawn out, probably because of a higher kinetic contribution in the electrode processes. For H_2O_2 concentrations of about 200 mM, in the anodic region, beyond the first plateau at about 0.6 V, the current drops suddenly (curve h). This phenomenon is accompanied by a general current decrease over the entire potential range explored. Further addition of H_2O_2 in the solution (up to about 500 mM) provided similar voltammetric behaviours, the current drop occurring at less positive potentials. Moreover, at the highest H_2O_2 concentration, strong current oscillations were observed at the anodic potentials. Under these conditions, the current response was no longer useful for analytical purposes (see later).

Calibration plots were obtained from current measurement both in the anodic and cathodic regions, over the concentration range where either a single or multiple waves were recorded. In the latter situations, the overall currents, corresponding to the second wave of each anodic or cathodic branch at a fixed and properly chosen potential, were considered. At least 10 points for each 10-fold H_2O_2 concentration change were considered. It was found that, the current responses were proportional to concentration for both anodic and cathodic branch, the slopes of the straight lines were very close to one another, and linearity extended even over the H_2O_2 concentration range where the phenomenon of the wave split occurred. These results, therefore, suggest that the same diffusing species is responsible of all waves observed in Fig. 4.

The general voltammetric behaviour described above was common for all Pt-Bs investigated. However, the wave split, the current drop phenomenon and consequently the linearity of calibration plots depended, other than on the H_2O_2 concentration, also on the phosphate buffer concentration as well

Table 2
Analytical characteristics of the Pt-Bs and H_2O_2 concentrations where the wave splits or current drop phenomena occur

Pt-B		Phosphate buffer c (M)	Calibration plot I_L (nA) = sC (mM) + q	R^2	Linear range (mM)	$C_{H_2O_2\ split}$ (±10 mM)	$C_{H_2O_2\ drop}$ (±10 mM)
RF	a (μm)						
31.9	13.7	0.2	I_L[a] = 11.3C + 16.2	0.999	0.1–180	100	200
			I_L[b] = 10.7C + 22.6	0.999	0.1–180	100	200
31.9	13.7	1	I_L[a] = 9.1C + 12.7	0.999	0.1–190	150	200
			I_L[b] = 8.5C + 15.6	0.999	0.1–180	150	200
10.1	12.7	1	I_L[a] = 12.1C − 16	0.999	0.1–80	150	200
			I_L[b] = 9.5C + 10.0	0.999	0.1–80	150	200
23.4	12.8	1	I_L[a] = 12.5C − 23	0.998	0.1–230	220	250
			I_L[b] = 8.8C + 13.0	0.999	0.1–200	200	300
50.5	14.2	1	I_L[a] = 9.3C + 11.1	0.999	0.1–180	150	200
			I_L[b] = 8.4C + 13.5	0.999	0.1–180	150	200
97.1	16.5	1	I_L[a] = 11.1C + 18.7	0.999	0.5–40	110	50
			I_L[b] = 10.9C + 12.5	0.999	0.5–40	120	50
3.6[c]	12.5	0.2	I_L[a] = 8.3C + 12.1	0.999	0.05–4.0	d	d
			I_L[b] = 8.1C + 11.4	0.999	0.05–4.0		

s = slope, q = intercept; d, no split or drop phenomena were observed.
[a] Anodic plateau.
[b] Cathodic plateau.
[c] Data for an uncoated Pt microdisk.

as on the RF factor of the Pt-Bs. Table 2 summarises typical calibration equations obtained by linear regression analysis of experimental data points, the linear dynamic ranges, the hydrogen peroxide concentrations at which the wave split ($C_{H_2O_2\ split}$) or current drop ($C_{H_2O_2\ drop}$) occurred for some of the Pt-Bs investigated in phosphate buffer solutions at different concentrations. From this table it is evident that the Pt-Bs with RF in the range 20–50 display good analytical performance. Moreover, for a given Pt-B, the $C_{H_2O_2\ split}$ is greater at higher buffer concentrations. $C_{H_2O_2\ drop}$, apart from the Pt-B of RF = 97, is over the range 200–300 mM. It must be considered that both $C_{H_2O_2\ split}$ and $C_{H_2O_2\ drop}$ values are not critical. They were observed within about 20 mM changes in H_2O_2 concentration.

In order to highlight the importance of the platinum black deposit and the high surface area that it provides, comparative measurements in H_2O_2 solutions were performed with an uncoated Pt microdisk, whose RF was about 4. Although also in this case a mixed anodic–cathodic wave (not shown) similar to those obtained at the Pt-Bs were recorded, the current–potential branches were less steep. As also evident from the analytical characteristics for the latter microelectrode included in Table 2, linearity between current against concentration was lost at a rather low hydrogen peroxide concentration value. Because of the low hydrogen peroxide concentration that can be explored with a smooth Pt disk, no wave split or current drop phenomena could be recorded before complete electrode surface saturation.

Surprisingly, the Pt-B with the largest surface area gave the worst analytical characteristics. Also, the current drop phenomenon appeared at H_2O_2 concentrations lower than those at which the wave split.

All the above results were rationalised considering the reaction mechanism reported in the literature, which was mentioned in the introduction section [28–32]. In fact, the rather large surface area of the Pt-Bs investigated here allows, in general, a large number of active sites to be formed, and consequently to improve the catalytic activity of Pt towards the H_2O_2 decomposition. Moreover, because of the high mass transport involved at the microelectrodes, both O_2 and H^+ reaction products could be efficiently removed from the electrode surface, thus making their inhibition reactions less effective. For these reasons, the linearity of calibration plots could be extended to rather high hydrogen peroxide concentrations, up to the remarkable value of 230 mM with the Pt-B of RF = 23.4 (Table 2).

The additional waves observed at the higher H_2O_2 concentrations could be explained by considering that, under the latter conditions, large amounts of hydrogen ions are involved either in the oxidation or reduction processes. Consequently, depending on the concentration of phosphate buffer in the medium, this may result in a strong decrease of the buffering capacity of the electrolyte within the platinum black pores. In particular, a local decrease of pH within the pore may cause the shift of each branch of the mixed wave towards more anodic and more cathodic potentials. This view is congruent with linear sweep and rotating disk experiments for H_2O_2 on platinum electrodes reported previously [23,24,31]. In fact, in those experiments it was found that as the pH of the bulk solution was decreased, the oxidation and reduction wave due to H_2O_2 became more anodic and cathodic, respectively. This is also a consequence of the dependence of the electrode reaction rate on pH of the medium [31].

Table 3
Diffusion coefficient of H_2O_2 and sensitivity obtained from current against concentration plots in phosphate buffer solutions at different concentrations

Phosphate buffer c (M)	D ($cm^2\ s^{-1}$)	Sensitivity ($A\ M^{-1}\ cm^{-2}$)
0.2	1.08×10^{-5} [a] (±0.13)	1.95[a]
	1.01×10^{-5} [b] (±0.01)	1.90[b]
1	0.97×10^{-5} [a] (±0.18)	2.00[a]
	0.82×10^{-5} [b] (±0.03)	1.85[b]
2.5	0.85×10^{-5} [a] (±0.05)	1.75[a]
	0.73×10^{-5} [b] (±0.04)	1.70[b]

[a] From anodic current.
[b] From cathodic current.

The hypothesis of insufficient buffering capacity of the medium at the vicinity of the electrode surface at high H_2O_2 concentrations is also supported by the experiments performed with a given Pt-B in phosphate buffers at different concentrations. In fact, as is evident from data shown in Table 2, for the Pt-B with RF = 32, $C_{H_2O_2\ split}$ is about 100 and 150 mM, for phosphate buffer concentration of 0.2 and 1 M, respectively. Also, as is illustrated in Fig. 4B, which contrasts typical voltammograms obtained with the Pt-B (RF = 32) in a 100 mM H_2O_2 solution containing either 0.2 or 1 M phosphate buffer, the wave splits in 0.2 M phosphate buffer, while a single mixed anodic–cathodic wave applies in 1 M buffer. The higher phosphate buffer concentration, however, led to an overall current decrease. This is probably related to the decrease of the diffusion coefficient of H_2O_2 as a consequence of the increase of the viscosity of the medium [52].

Apparent diffusion coefficient values for a range of phosphate buffer concentrations were evaluated from the slopes of the calibration plots (both from anodic and cathodic currents), and the average data obtained from all Pt-Bs are shown in Table 3. As expected, the diffusion coefficient decreases as the concentration of the base electrolyte increases, in accordance with the above-mentioned effect of the viscosity of the base electrolyte. Moreover, the diffusion coefficient values found here in 0.2 and 1 M buffer are well within those recently quoted in the literature, which range between 0.6×10^{-5} and $1.46 \times 10^{-5}\ cm^2\ s^{-1}$ [23,28,42].

The sudden current drop phenomenon in the more concentrated hydrogen peroxide solutions (Fig. 3A, curve h) was explained considering that a large amount of oxygen bubbles are also formed within the platinum black pores during the oxidation process. This from one side could limit the diffusion of H_2O_2 towards the active sites of the Pt-B; from the other, the enhanced oxygen concentration within the pore could induce saturation of available binding sites [28–31]. Based on the wave shape in Fig. 3A (curve h), we believe the first situation to be prevailing.

As is evident from data of Table 2, $C_{H_2O_2\ drop}$ depends on the RF of the electrode, and it is relatively low for the Pt-B with the highest roughness factor. This is probably related to the fact that the larger the amount of platinum black deposited the more disordered is its pore structure. This in turn would make the accessibility of the analyte to the active sites less easy.

The latter considerations may also account for the general poorer analytical characteristics of the Pt-B with the highest RF factor. In fact, the non-regular pore distribution of the platinum black deposit may strongly limit diffusion either of H_2O_2 down the pores or O_2 and H^+ out from them. This causes all the above discussed detrimental factors for current versus concentration linear dependence, wave split and current drop to be enhanced. Nevertheless, even with the largest platinum black deposit, linear calibration plots up to about 40 mM could be achieved.

It must be remarked that the general performance of the smooth Pt microdisk, as expected, are by far lower than those of any Pt-Bs investigated here and therefore it is not useful for the detection of concentrated hydrogen peroxide solutions.

3.3. Repeatability, electrode stability, sensitivity and lower detection limits

Replicate measurements (n = 6–8) performed with the same Pt-B at a given H_2O_2 concentration (within the linear range) displayed high reproducibility (within 2%), regardless of RF. The stability of the electrodes was investigated by monitoring a 50 mM H_2O_2 solution during a working day (8 h). In all cases, the voltammograms and in particular the current signals appeared stable (within 3%). Moreover, the same electrode could be used with almost identical performance for about 10 days. After this period, a series of measurements was performed to check whether variation of the Pt-Bs electrode radii and RF factors occurred. It was found that the latter parameters decreased by no more than 10% with respect to the initial values. This indicates that the Pt-Bs also possess a rather good stability.

Sensitivity was calculated by the slope of each calibration curve (both from anodic and cathodic current) in the linear range. Table 3 includes the best values found at different phosphate buffer concentrations. As is evident the cathodic currents provided lower sensitivities. However, the average value 1.93(±0.06) $A\ M^{-1}\ cm^{-2}$, calculated from those found in phosphate buffers up to 1 M, is within the highest reported in the literature, i.e., 1–2.8 $A\ M^{-1}\ cm^{-2}$ [13,42] with amperometric devices.

Finally, low detection limits, based on the signal to noise ratio equal to 3 were evaluated, and the best value of 0.05 mM was found using the Pt-Bs with RF of 10.1 and 23.4.

3.4. Application to a real sample

To investigate the actual applicability of the Pt-Bs to practical usage, the H_2O_2 concentration of a commercial antiseptic solution was determined. In particular, a solution for so-called clean-in-place process of bottle beverages [53] was analysed. On the typical sterilisation process, the original (as provided by the supplier) antiseptic solution is diluted with pure water by about 30–50-fold. Since the latter solutions still

Table 4
Results of the determination of H_2O_2 in an antiseptic solution by voltammetry using a Pt-B with RF = 32, and by titration with $KMnO_4$

Diluted antiseptic sample	I_L (±10 nA)[a]	I_L (±10 nA)[b]	C[c] (mM) [R.S.D.%]	C[d] (mM) [R.S.D.%]
1	650	1110	72.5 [1.6]	75.7 [1.2]
2	490	960	54.5 [1.5]	51.7 [1.3]

[a] Blank current.
[b] Sample spiked with 50 mM H_2O_2.
[c] From anodic current.
[d] From titration with $KMnO_4$. [R.S.D.] = relative standard deviation from four replicates.

contain rather high H_2O_2 concentrations (larger than those for which linearity applies for the Pt-Bs employed here), a further dilution with Milli-Q water was necessary to bring the hydrogen peroxide content within those shown in Table 1. Moreover, a phosphate buffer, to maintain the solution pH to about 7, was also added to the samples. The Pt-B employed for these experiments had RF = 32.

Cyclic voltammetry at low scan rates was performed on the diluted solutions and voltammograms similar to those shown in Fig. 4 were obtained. The anodic current at 0.80 V versus PtPRe was used for evaluating the H_2O_2 concentration. Trials on each sample tested, using the standard addition method, were carried out four times. In each case the addition of a known amount of hydrogen peroxide was made in order to increase the initial concentration as ≈2-fold (i.e., about twice the blank current). The average concentration values thus evaluated were compared with those obtained by the conventional redox titration using $KMnO_4$ [11]. Table 4 summarises all experimental data obtained from the above experiments. As is evident concentration data obtained by the two procedures are satisfactory, the agreement being within 6%.

4. Conclusions

The results obtained in this paper have shown that platinum black coated microelectrodes provide a means to improve sensibly the upper detection limits for hydrogen peroxide determinations. In fact with these electrode systems, H_2O_2 concentrations up to 230 mM can be determined, provided that the roughness of the electrode and the phosphate buffer concentration are properly designed. In fact, a high surface area of the electrode is needed to make the number of binding sites (responsible for the enhanced catalytic activity of Pt for the H_2O_2 decomposition to O_2 and H_2O) large enough, thus avoiding saturation phenomena. Pt-Bs with RF in the range 20–50 have provided satisfactory analytical performance. On the other hand, as the overall electrode process is affected by local change of pH (according to reactions (2) and (3)), at higher hydrogen peroxide concentrations, a lost of the buffering capacity of the base electrolyte may be induced. Under these conditions, a sufficiently high concentration of phosphate buffer is required to avoid either inhibition of the active sites by their protonation, or shift of the oxidation–reduction waves to more positive or more negative potential values. Local decrease of pH may lead to additional waves, which however if included in the calibration plots did not affect their linearity. The average sensitivity of 1.93(±0.06) A M^{-1} cm^{-2} found here with the various Pt-Bs is comparable to other electrode systems. However, because of the high surface area and the relatively larger background currents of the Pt-Bs, low detection limits are less improved. In fact, based on signal to background noise of 3, a low detection limit of 0.05 mM was established with a Pt-B of relatively low roughness factors.

Acknowledgement

Financial support by MIUR, Rome is gratefully acknowledged.

References

[1] F.A. Armstrong, G.S. Wilson, Electrochim. Acta 45 (2000) 2623.
[2] K. Schliefer, G. Heidemann, Melliand Textilberichte 70 (1989) 856.
[3] P. Westbroek, E. Temmerman, P. Kiekens, Anal. Chim. Acta 385 (1999) 423.
[4] P. Westbroek, B. van Haute, E. Temmerman, Fresen. J. Anal. Chem. 354 (1996) 405.
[5] M. Fagan, J.R. Walton, U.S. Peroxide 949 (1999) 661.
[6] D. Suznjevic, S. Blagojevic, D. Vucelik, P. Zuman, Electroanalysis 9 (1997) 861.
[7] P. Trinder, Ann. Clin. Biochem. 6 (1969) 24.
[8] C. Matsubara, K. Kudo, T. Kawashita, K. Takamura, Anal. Chem. 57 (1985) 1107.
[9] K. Nakashima, K. Maki, S. Kawaguchi, S. Akyima, Y. Tsukamoto, I. Kazuhiro, Anal. Sci. 7 (1991) 709.
[10] A.L. Lazurua, G.L. Kok, S.N. Gitlin, J.A. Lind, S.E. Mclaren, Anal. Chem. 57 (1985) 917.
[11] A.J. Vogel, Textbook of Quantitative Inorganic Analysis, Longman, New York, 1978.
[12] M. Vreeke, R. Maidan, A. Heller, Anal. Chem. 64 (1992) 3084.
[13] T. Ruzgas, E. Csoregi, J. Emneus, L. Gorton, G. Marko-Varga, Anal. Chim. Acta 330 (1996) 123.
[14] M. Gerlache, S. Girousi, G. Quarin, J.M. Kauffmann, Electrochim. Acta 43 (1998) 3467.
[15] M. Gerlache, Z. Senturk, G. Quarin, J.M. Kauffmann, Electroanalysis 9 (1997) 1088.
[16] Y. Zhang, G. Wison, J. Electroanal. Chem. 345 (1993) 253.
[17] D.A. Johnston, M.F. Cardosi, D.H. Vaughan, Electroanalysis 7 (1995) 520.
[18] J.A. Cox, R.K. Jaworski, Anal. Chem. 61 (1989) 2176.
[19] T. You, O. Niwa, M. Tomita, S. Hirono, Anal. Chem. 75 (2003) 2080.
[20] K. Aoki, M. Ishida, K. Tokuda, K. Hasebe, J. Electroanal. Chem. 251 (1988) 63.
[21] W.B. Nowall, W.G. Kuhr, Electroanalysis 9 (1997) 102.
[22] T. Imato, H. Ohura, S. Yamasaki, Y. Asano, Talanta 52 (2000) 19.
[23] V.G. Prabhu, L.R. Zarapkar, R.G. Dhaneshwar, Electrochim. Acta 26 (1981) 725.
[24] G.G. Guilbault, G.J. Lubrano, Anal. Chim. Acta 64 (1973) 439.

[25] Y. Ikaryama, S. Yamauchi, T. Yukiashi, H. Ushioda, Anal. Lett. 20 (1987) 1407.
[26] Y. Ikaryama, S. Yamauchi, T. Yukiashi, H. Ushioda, Anal. Lett. 20 (1987) 1791.
[27] J. Wang, J. Pharmaceut. Biomed. 19 (1999) 47.
[28] S.B. Hall, E.A. Khudaish, A.L. Hart, Electrochim. Acta 43 (1998) 579.
[29] S.B. Hall, E.A. Khudaish, A.L. Hart, Electrochim. Acta 43 (1998) 2015.
[30] S.B. Hall, E.A. Khudaish, A.L. Hart, Electrochim. Acta 44 (1999) 2455.
[31] S.B. Hall, E.A. Khudaish, A.L. Hart, Electrochim. Acta 44 (1999) 4573.
[32] S.B. Hall, E.A. Khudaish, A.L. Hart, Electrochim. Acta 45 (2000) 3573.
[33] O. Niwa, T. Oriuchi, M. Morita, T. Huang, P.T. Kissinger, Anal. Chim. Acta 318 (1996) 167.
[34] J.I. Reyes De Corcuera, R.P. Cavalieri, J.R. Powers, Synth. Met. 142 (2004) 71.
[35] S. Hrapovic, Y. Liu, K.B. Male, J.H.T. Luong, Anal. Chem. 76 (2004) 1083.
[36] J. Wang, N.V. Myung, M. Yun, H.G. Monbouqette, J. Electroanal. Chem. 575 (2005) 139.
[37] E.E. Ferapontova, V.G. Grigorenko, A.M. Egorov, T. Borchers, T. Ruzgas, L. Gorton, Biosens. Biolectron. 16 (2001) 147.
[38] M.P. O'Halloran, M. Pravda, G.G. Guilbault, Talanta 55 (2001) 605.
[39] A.A. Karyakin, E.A. Puganova, I.A. Budashov, I.N. Kurochkin, E.E. Karyakina, V.A. Levchenko, V.N. Matveyenko, S.D. Varfolomeyev, Anal. Chem. 76 (2004) 474.
[40] M. Delwaux, A. Walcarius, S. Demoustier-Champagne, Anal. Chim. Acta 525 (2004) 221.
[41] M.E. Sandison, N. Anicet, A. Glidle, J.M. Cooper, Anal. Chem. 74 (2002) 5717.
[42] S.A.G. Evans, J.M. Elliot, L.M. Andrews, P.N. Bartlett, P.J. Doyle, G. Denuault, Anal. Chem. 74 (2002) 1322.
[43] B. Gollas, J.M. Elliot, P.N. Bartlett, Electrochim. Acta 45 (2000) 3711.
[44] N. Teshima, Z. Genfa, P.K. Dasgupta, Anal. Chim. Acta 510 (2004) 9.
[45] M.I. Montenegro, M.A. Queiros, J.L. Daschbach, Microelectrodes: Theory and Applications, NATO ASI Series, vol. E197, 1991.
[46] M.E. Abdelsalam, G. Denuault, M.A. Baldo, C. Bragato, S. Daniele, Electroanalysis 13 (2001) 289.
[47] Y. Saito, Rev. Polarogr. 15 (1968) 177.
[48] P. Sun, Z. Zhang, J. Guo, Y. Shao, Anal. Chem. 73 (2001) 5346.
[49] E. Levia, Electrochim. Acta 41 (1996) 2185.
[50] M. Noel, K.I. Vasu, Cyclic Voltammetry and the Frontiers of Electrochemistry, Aspect Publications Ltd., London, 1990, p. 347.
[51] S. Trasatti, O.A. Petrii, J. Electroanal. Chem. 327 (1992) 353.
[52] J.O. Bockris, A.K.N. Reddy, Modern Electrochemistry, vol. 1, Plenum Press, New York, 1970.
[53] P.A. Lynam, J.R. Babb, A.P. Fraise, J. Hosp. Infect. 30 (1995) 237.